



**HAL**  
open science

# Multifunctional Anthracene-Based Ni-MOF with Encapsulated Fullerenes: Polarized Fluorescence Emission and Selective Separation of C 70 from C 60

Serhii Vasylevskyi, Guillaume Raffy, Stefan Salentinig, André del Guerzo, Katharina Fromm, Dario Bassani

► **To cite this version:**

Serhii Vasylevskyi, Guillaume Raffy, Stefan Salentinig, André del Guerzo, Katharina Fromm, et al.. Multifunctional Anthracene-Based Ni-MOF with Encapsulated Fullerenes: Polarized Fluorescence Emission and Selective Separation of C 70 from C 60. ACS Applied Materials & Interfaces, 2022, 14 (1), pp.1397-1403. 10.1021/acsami.1c19141 . hal-03853623

**HAL Id: hal-03853623**

**<https://hal.science/hal-03853623>**

Submitted on 23 Nov 2022

**HAL** is a multi-disciplinary open access archive for the deposit and dissemination of scientific research documents, whether they are published or not. The documents may come from teaching and research institutions in France or abroad, or from public or private research centers.

L'archive ouverte pluridisciplinaire **HAL**, est destinée au dépôt et à la diffusion de documents scientifiques de niveau recherche, publiés ou non, émanant des établissements d'enseignement et de recherche français ou étrangers, des laboratoires publics ou privés.

# Multifunctional anthracene-based Ni-MOF with encapsulated fullerenes: polarized fluorescence emission and selective separation of C<sub>70</sub> from C<sub>60</sub>

*Serhii I. Vasylevskiy<sup>†‡\*</sup>, Guillaume Raffy<sup>‡</sup>, Stefan Salentinig<sup>†</sup>, André Del Guerso<sup>‡</sup>, Katharina M. Fromm<sup>†\*</sup> and Dario M. Bassani<sup>‡\*</sup>*

<sup>†</sup>Chemistry Department, University of Fribourg, Chemin du Musée 9, Fribourg, 1700, Switzerland.

<sup>‡</sup>University of Bordeaux, ISM CNRS UMR 5255, 33400, Talence, France.

**ABSTRACT:** We report an anthracene-based Ni-MOF (Ni(II) metal-organic framework, {[Ni( $\mu_2$ -**L**)<sub>2</sub>Cl<sub>2</sub>] $\cdot$ *x*(C<sub>6</sub>H<sub>6</sub>) $\cdot$ *y*(MeOH)]<sub>n</sub> (**1**), **L** = anthracene-9,10-diylbis(methylene)diisonicotinate) whose crystal structure reveals the presence of hexagonal channels with a pore size of 1.4 nm that can accommodate guests such as C<sub>60</sub> and C<sub>70</sub>. Both confocal fluorescence and Raman microscopy results are in agreement with a homogeneous distribution of fullerenes throughout the single crystals of **1**. Efficient energy transfer from **1** to the fullerenes was observed, which emitted partially polarized fluorescence emission. Stronger binding between **1** and C<sub>70</sub> vs. C<sub>60</sub> was confirmed from HPLC analysis of the dissolved material and provides a basis for the selective retention of C<sub>70</sub> in liquid chromatography columns packed with **1**.

KEYWORDS: Metal-organic frameworks (MOFs), self-assembly Ni-MOFs, fullerenes encapsulation, C<sub>60</sub>/C<sub>70</sub> separation, energy transfer, polarized emission.

## INTRODUCTION

The synthesis of new metal-organic frameworks (MOFs) is highly promising for potential applications in fields such as catalysis, gas storage and separation, light harvesting materials, and medicine.<sup>1-10</sup> For example, encapsulation of small guests such as quantum dots or organic dyes in the pores of MOFs have resulted in new materials for applications in drug delivery,<sup>11,12</sup> tunable light emission,<sup>4,5,13,14</sup> LEDs,<sup>6</sup> sensing and recognition,<sup>7</sup> magnetism<sup>8</sup> and up-conversion of light.<sup>9,10</sup> Roswell and Yaghi proposed that impregnation of fullerenes in MOFs will increase their specific surface area for molecular hydrogen storage applications by introducing additional sorptive sites inside the pores.<sup>15</sup> Subsequent studies in this direction were aimed at encapsulation of fullerenes such as C<sub>60</sub> and C<sub>70</sub> into MOFs using the soaking method, in which interaction of fullerene molecules occurs from a solution in contact with the MOF.<sup>16,17</sup> Thus, MIL-101(Cr) was shown to separate fullerene mixtures C<sub>60</sub>/C<sub>70</sub> via surface interactions.<sup>18,19</sup> The interaction of fullerene molecules with the surface of a MOF furthermore enhanced its electrical conductivity<sup>20</sup> or the molecular recognition properties<sup>21</sup> of the material. However, achieving a homogeneous distribution of fullerene guest molecules within a mesoporous solid remains a major challenge compounded by the difficulty in differentiating between migration into the pores or localization on the MOF surface.

Previous results suggesting successful encapsulation of fullerenes inside of MOFs obtained using the soaking approach relied on powder X-ray diffraction (PXRD) or Raman spectroscopy to ascertain the presence of trapped fullerenes such as C<sub>60</sub>.<sup>22,23</sup> However, these techniques are not sufficient to confirm the sorption of the fullerenes deep into the pores of a MOF. We believe that

the encapsulation of fullerenes by MOFs by using a soaking approach is generally rather limited: soaking leads mainly to the deposition of fullerenes on the outer MOF surface and the deep diffusion of fullerenes from the solution into the pores of MOF is less likely.<sup>24</sup> This limitation is often caused by e.g. trapped solvents inside of the MOF pores that prevent the larger guests such as fullerenes to diffuse and be encapsulated.<sup>24</sup> This issue was also observed for more robust systems such as zeolites with encapsulation of the organic dyes.<sup>25,26</sup> Imahori and co-workers achieved a constant loading of C<sub>60</sub> fullerene throughout a phthalocyanine-based material using a layer-by-layer process.<sup>24</sup> In contrast to the self-assembled MOFs with fullerenes, this process is carried out in the presence of dissolved fullerenes, and encapsulation occurs in a homogeneous manner since it is not limited by diffusion throughout the material.

Herein, we report the assembly of an anthracene-based Ni(II)-MOF (**1**) that encapsulates C<sub>60</sub> and C<sub>70</sub> fullerenes inside 1D channels. In contrast to previous reports of fullerene-impregnation of freestanding MOFs, the integration of fullerenes into **1** was accomplished during the self-assembly process of the MOF itself. Hybrid C<sub>60</sub>@Ni-MOF (**2**) and C<sub>70</sub>@Ni-MOF (**3**) exhibit interesting optical properties such as the observation of linearly polarized light resulting from the arrangement of the guest molecules inside the 1D channels. Energy transfer from the anthracene chromophores in **1** to the encapsulated fullerenes acceptors is particularly efficient and can be used to probe the distribution of the fullerenes in single crystals of **1** using confocal fluorescence microscopy (CFM). Both CFM and confocal Raman microscopy (CRM) show that the distribution of the fullerenes in single crystals of Ni-MOF is constant throughout the entire crystal matrix, in agreement with a homogenous distribution of fullerenes in C<sub>60</sub>@Ni-MOF (**2**) and C<sub>70</sub>@Ni-MOF (**3**). Furthermore, the rigid structure of **1** allows it to discriminate between C<sub>60</sub> and C<sub>70</sub>, allowing their separation based on their dimensions.

## EXPERIMENTAL

Materials and methods. Reagents were used as obtained without further purification: NiCl<sub>2</sub>·6H<sub>2</sub>O, methanol and reagent grade benzene were obtained from Merck (Sigma-Aldrich), C<sub>60</sub> and C<sub>70</sub> with purity 99.9% were received from TCI, the fullerene mixture was obtained from MTR with 75% and 25% C<sub>60</sub>:C<sub>70</sub> based on HPLC analysis. HPLC analyses were performed using a Waters high performance liquid chromatograph equipped with a diode array UV-vis detector (200-900 nm), a modified reverse silica C18 column (COSMOSIL Buckyprep, 5 μm, 4.6 mm I.D. x 250 mm) eluted with acetonitrile and toluene (40:60). The fullerene signal was monitored at 325 nm. Solid-state absorption spectra were collected on a Perkin Elmer UV/VIS/NIR Lambda 900 using an integrating sphere in reflection mode. IR absorption spectra were recorded on a Perkin Elmer FT-IR spectrometer Frontier 4000-400 cm<sup>-1</sup>, with golden-gate geometry. Single crystal diffraction data (SXRD) were obtained from a STOE-IPDS II (Single crystal diffractometer λ-Mo, Kα radiation, λ = 0.71073 Å). Thermal analyses (TGA) were performed at a heating rate of 10°C min<sup>-1</sup> from 20 to 600°C in a Mettler Toledo SDTA 851a. Powder diffraction XRD (PXRD) investigations were carried out on a STOE STADI P diffractometer with Cu Kα (λ=1.5406 Å) radiation. Elemental analyses for C, H and N were carried out using a FLASH 2000 Organic Elemental Analyzer.

Synthesis of Ni-MOF (**1**), C<sub>60</sub>@Ni-MOF (**2**) and C<sub>70</sub>@Ni-MOF (**3**). A methanol solution (5 mL) containing NiCl<sub>2</sub>·6H<sub>2</sub>O (23.7 mg 0.1 mmol) was layered over a solution of benzene (15 mL) containing anthracene-9,10-diylbis(methylene)diisonicotinate (**L**) (89.6 mg, 0.2 mmol). The mixture was left to diffuse for a week, resulting in hexagonal tipped green needles suitable for SXRD (See SI) with a yield of ca. 98%. Calc. for C<sub>68</sub>H<sub>52</sub>Cl<sub>2</sub>N<sub>4</sub>NiO<sub>8</sub> (**1**): C, 69.05; H, 4.43; N, 4.73. Found: C, 79.56; H, 5.00; N, 4.09 – corresponding to the formula C<sub>81</sub>H<sub>68</sub>Cl<sub>2</sub>N<sub>4</sub>NiO<sub>9</sub>: {[Ni(μ<sub>2</sub>-**L**)<sub>2</sub>Cl<sub>2</sub>]·4(Benzene)·1(MeOH)}<sub>n</sub> (**1**) (air-stable form). Compounds **2** and **3** were synthesized by

using similar protocol as for **1** by first dissolving 1 mg of either C<sub>60</sub> (1.38 mmol) or C<sub>70</sub> (1.19 mmol) in 15 mL of benzene. The mixture was stirred until full dissolution, after which 0.2 mmol of anthracene-9,10-diylbis(methylene)diisonicotinate (89.6 mg) was added and stirred for another 25 min until complete dissolution of the ligand. Then, 0.1 mmol of NiCl<sub>2</sub> hexahydrate (23.7 mg) was dissolved in 5 mL of methanol and layered on top of the benzene solution. After complete self-diffusion over one week, dark-brown C<sub>60</sub>@Ni-MOF (**2**) or brown crystals C<sub>70</sub>@Ni-MOF (**3**) were obtained with yields of 96 – 98%. CCDC numbers 1977368 for C<sub>60</sub>@Ni-MOF (**2**) and 1977380 for C<sub>70</sub>@Ni-MOF (**3**). Binary ratios of C<sub>60</sub>:C<sub>70</sub> (90:10, 75:25, 50:50; 25:75, and 10:90)@Ni-MOF were synthesized similarly as for **2** or **3**, but using a solution containing varying proportions of C<sub>60</sub>:C<sub>70</sub> (1 mg of fullerene mixture for 15mL of benzene). In all cases, brown single crystals were obtained and used for further analyses. Additional experimental details are provided in the supporting information file.

## RESULTS AND DISCUSSION

The Ni-MOF {[Ni( $\mu_2$ -L)<sub>2</sub>Cl<sub>2</sub>].x(C<sub>6</sub>H<sub>6</sub>).y(MeOH)}<sub>n</sub> (**1**) was obtained using the ligand anthracene-9,10-diylbis(methylene)diisonicotinate (**L**) and NiCl<sub>2</sub>·6H<sub>2</sub>O in MeOH/benzene as solvents (Figure 1a). Ni-MOF **1** crystallizes in the non-centrosymmetric space group *P*6<sub>4</sub>22 and has a hexagonal structure similar to hexagonal mesoporous silica.<sup>27</sup> It presents two types of 1D continuous channels running along the *c*-axis: one with diameter of 8.1 Å (C2...C10) and the other with 15.6 Å diameter (O2...O2'), measured as the diagonal using van der Waals radii of the atoms (Figure 1c). The channels result from the helical structure formed by coordination of bridging **L** to NiCl<sub>2</sub> nodes (Figure 1b). During the coordination of **L** to Ni<sup>2+</sup>, torsion of the O–CH<sub>2</sub> bond of the isonicotinate groups with respect to the anthracene moiety induces helical chirality. In **1**, each nickel (II) ion is

coordinated by four ligands **L** and two axially positioned chloride ions, leading to an octahedral coordination.

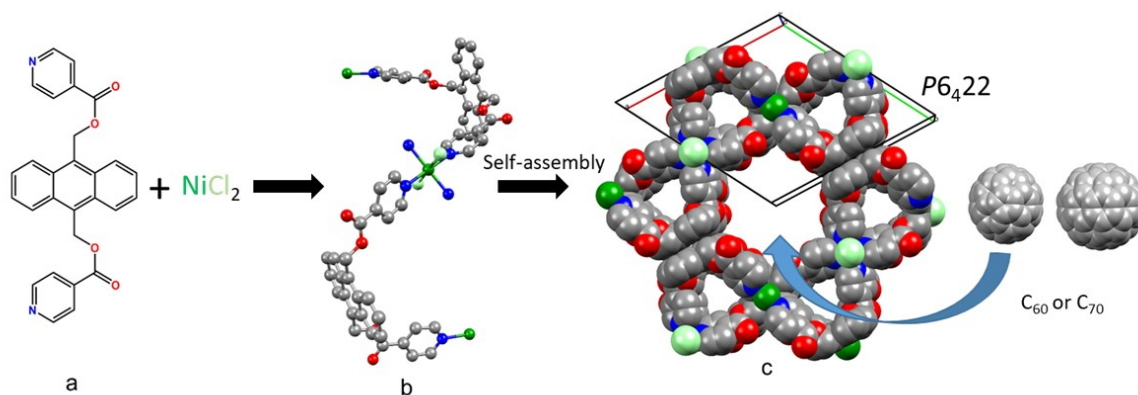


**Figure 1.** Synthesis of Ni-MOF **1** showing the conformational rearrangement of the ligand leading to the helical structure of the Ni-MOF assembly and view along the *c*-axis in the crystal structure of **1** revealing a hexagonal architecture and projection along the two types of pores with  $\varnothing$  15.6 Å and 8.1 Å. Encapsulation of fullerenes is proposed to occur in the larger pore. (Hydrogen atoms are omitted for clarity).

The presence of dissolved guests such as  $C_{60}$  or  $C_{70}$  during the self-assembly of **1** leads to the inclusion of fullerene molecules into the larger pores. As a consequence, whereas preparation of **1** in benzene results in the formation of a greenish solid typical of Ni(II) salts, the presence of either  $C_{60}$  or  $C_{70}$  in solution affords brown crystals as a result of the formation of  $C_{60}$ @Ni-MOF (**2**) or  $C_{70}$ @Ni-MOF (**3**), respectively (Figure 2). Single crystal diffraction from **2** and **3** indicate that both possess the same framework structure as **1**, with no significant changes in the cell parameters (Table S1). This suggests that inclusion of the fullerene cage does not template the self-assembly of **1**, and that the resulting inclusion complexes may possess higher loading ratios than would have been possible by soaking. The single crystals of **2** and **3** give non-constructive/destructive diffraction patterns of fullerenes inside the Ni-MOF,<sup>28</sup> presumably due to the absence of symmetry between trapped fullerenes in the 1D channels of Ni-MOF. The fullerenes are expected to have a high degree of rotational freedom and to be randomly oriented inside the channels. Similar studies

for MIL-101(Cr) and NU-901 showed large broadening of the X-ray diffraction peaks after soaking with fullerenes,<sup>18,24,29</sup> which was attributed to the deposition of the fullerenes on the particles' outer surface with concomitant reduction and broadening of MOF-lattice's diffraction peaks.<sup>18,24,29</sup> In contrast, the powder x-ray diffraction patterns for both **2** and **3** give narrow diffraction peaks consistent with homogeneously distributed fullerenes, supporting the conclusion that the fullerenes are not located solely on the surface, but distributed regularly throughout the crystallites of **2** and **3** (Figure S1).

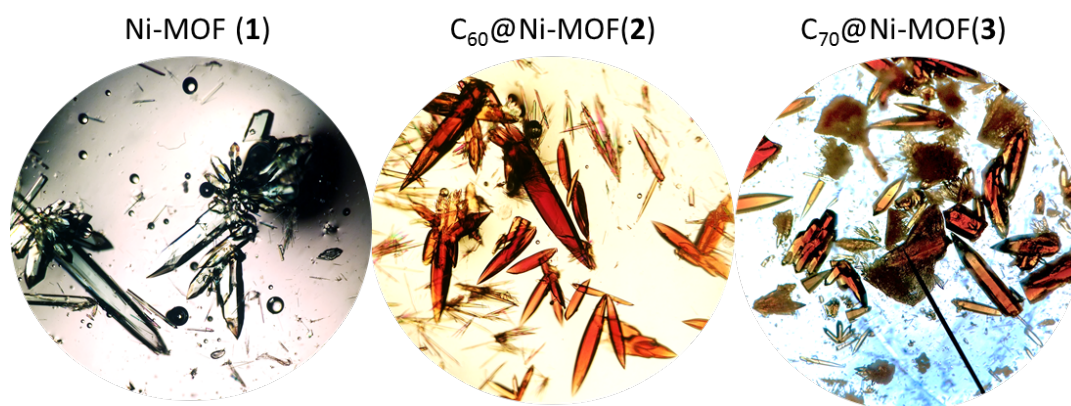


**Figure 2.** Optical microscope images of Ni-MOF (**1**), C<sub>60</sub>@Ni-MOF (**2**) and C<sub>70</sub>@Ni-MOF (**3**) at 10× magnification.

In order to better analyze the homogeneity of the encapsulation of the fullerenes in **1**, the Raman signals of the entrapped fullerenes as a function of penetration depth in single crystals was collected using confocal Raman microscopy using 785 nm laser excitation (Figure 3a - 3f). The signals of the Ni-MOF (432 cm<sup>-1</sup>), of C<sub>60</sub> (491 cm<sup>-1</sup>, A<sub>g</sub>(1)) and of C<sub>70</sub> (452 cm<sup>-1</sup>, A<sub>1</sub>') were analyzed throughout the cross-section of the crystals (Figure 3c, 3f). In all crystals analyzed, the signal ratios between the signal intensity for C<sub>60</sub> (or C<sub>70</sub>) and those for the Ni-MOF lattice do not change significantly, indicating a homogenous distribution of the guest molecules throughout the single crystals of **2** (or **3**).

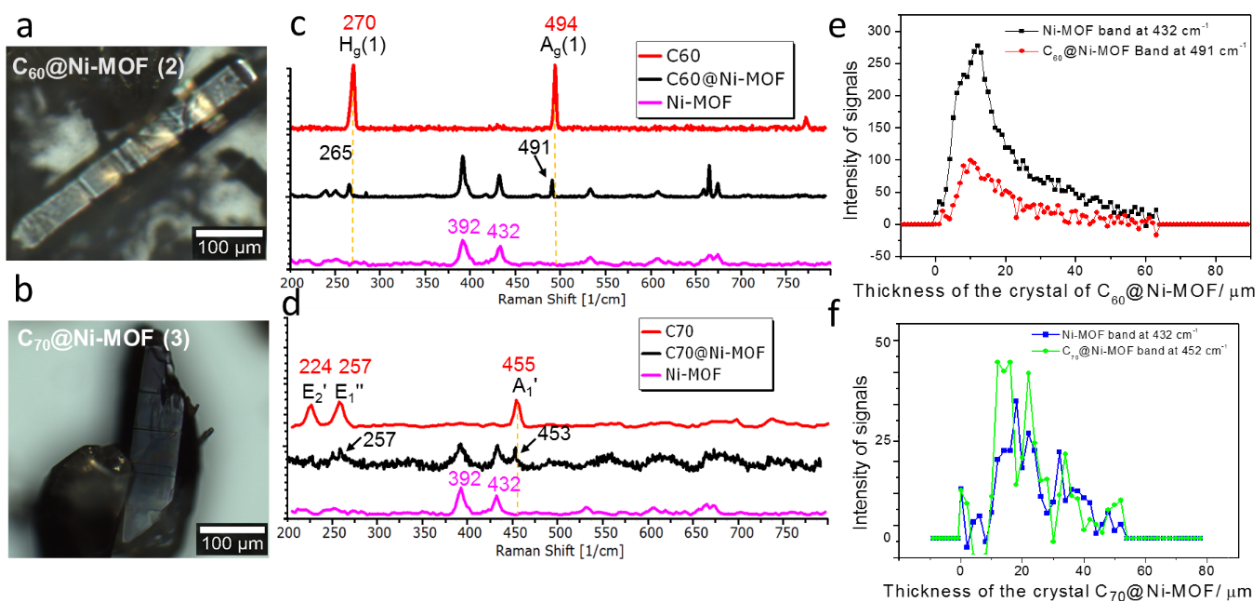


**Figure 3.** Single crystals of  $C_{60}@Ni-MOF$  (**2**) and  $C_{70}@Ni-MOF$  (**3**) (panels (a) and (b), respectively) and Raman spectra comparing the signals obtained from these crystals and those of **1** or  $C_{60}$  (c) or  $C_{70}$  (d). The intensity of the Raman signal of the encapsulated fullerene and of **1** measured along the crystal's cross-section is shown in (e) and (f) for **2** and **3**, respectively (785 nm excitation laser with 5  $\mu m$  steps).

Numerous studies have shown that supramolecular organization can strongly impact the electronic properties of individual chromophores.<sup>30</sup> To probe the effect of organization on the electronic properties of the fullerenes in **2** or **3**, we used confocal fluorescence microscopy to examine different parts of single crystals. Probing the fullerene emission from different positions along the  $z$ -axis of **2** or **3** gives nearly identical fluorescence spectra, intensity, and decay parameters. This shows that encapsulation of  $C_{60}$  and  $C_{70}$  is homogeneous with respect to the resolution of the instrument (ca. 700 nm in the  $z$ -axis, Figure 4a and 4b). As shown in Figure 4, excitation of **2** and **3** at 375 nm, where both **1** and the fullerenes absorb, leads to the detection of the emission from the anthracene moiety of the Ni-MOF (400 – 550 nm) as well as weaker emission from the encapsulated  $C_{60}$  and  $C_{70}$  (650 – 850 nm). Emission spectra of the single crystals of **2** and **3** obtained upon excitation at 450 nm, where only  $C_{60}$  or  $C_{70}$  absorb, leads to the expected

broad emission at 650 – 850 nm attributed to the fullerene molecules (Figure 4). The emission spectrum from encapsulated  $C_{60}$  in **2** presents a single emission band with a maximum at 690 nm originating from anisotropic electronic transitions, in contrast to  $C_{70}$  (**3**), which shows a sharp band at 670 nm and additional shoulders at 695 nm and 722 nm. Well-resolved emission from  $S_1^*$  in  $C_{70}$ .<sup>31–33</sup> is typically observed from frozen solutions or in matrices, suggesting that the incorporation of  $C_{60}$  or  $C_{70}$  into **1** does not lead to broadening of the  $S_1 \rightarrow S_0$  electronic transitions due to the solvent environment. Although we cannot rule out interaction between the fullerene and solvent molecules trapped in the channels of Ni-MOF, their effect on broadening the fullerenes' emission spectrum is apparently less than what is observed in solution.<sup>32</sup>

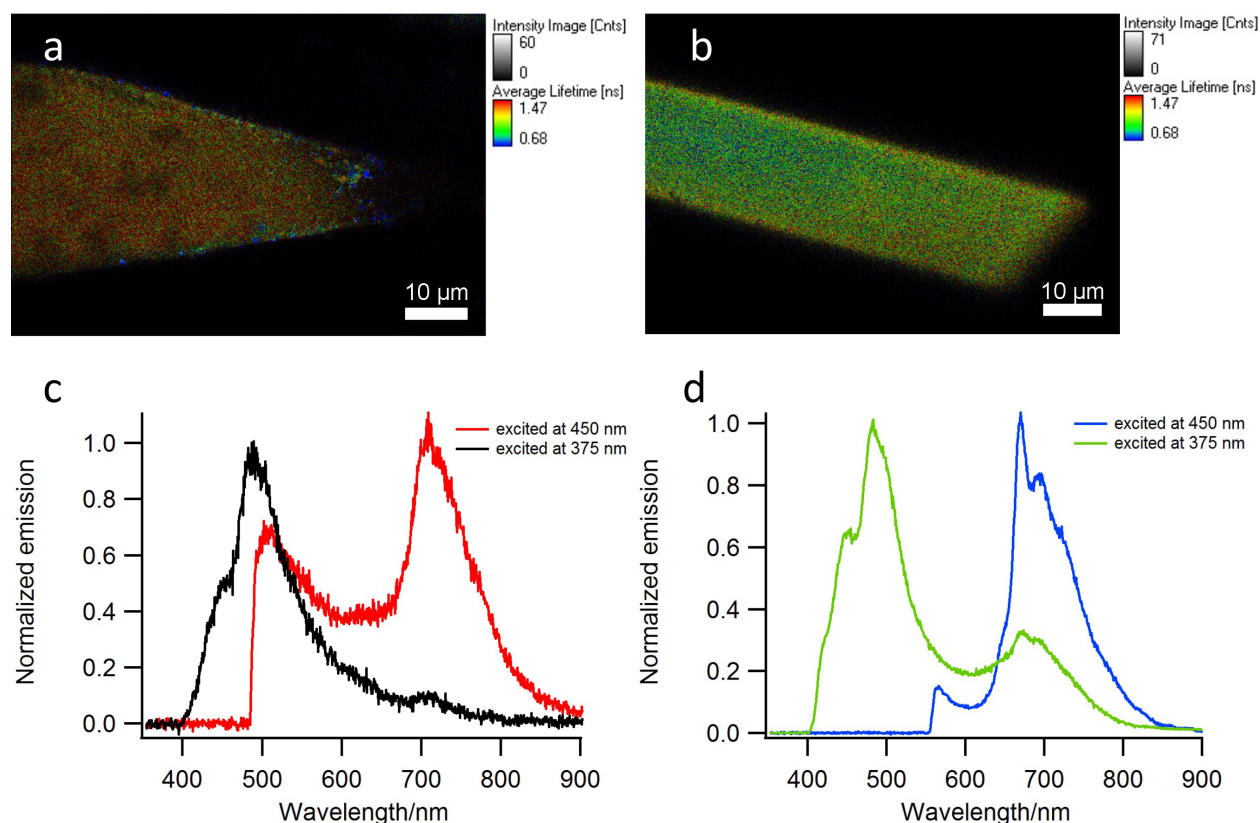


**Figure 4.** Fluorescence lifetime images from single crystals of **2** (a) and **3** (b). Emission spectra collected from single crystal of **1** with encapsulated  $C_{60}$  (c) and  $C_{70}$  (d) upon excitation of the anthracene chromophore in the MOF (at 375 nm) or of the fullerene (at 450 nm).

Analyzing the emission spectra from the encapsulated fullerenes  $C_{60}$  and  $C_{70}$  in **2** and **3** evidences that the fullerene emission exhibits linear polarization orientated with respect to the crystal alignment (Figure 5 a - f) and independent of the polarization of the excitation beam. Both **2** and **3** show emission that is partially oriented along the direction of the longest dimension of the crystal which, based on a fully indexed single crystal of **1**, is aligned with the  $c$ -axis of the unit cell. This in turn corresponds to the orientation of the 1D channels in the MOF (Fig. S2). Whereas such behavior is typical of chromophores whose electronic transition dipole moment associated with the lowest energy transition is oriented, it is absent in fullerenes due to their high degree of symmetry. In fact, polarized emission from fullerene materials was previously only documented in linear supramolecular aggregates possessing exciton delocalization over two or more  $C_{60}$  chromophores.<sup>22,34</sup> In this case, however, it is accompanied by significant bathochromic shift of the emission wavelength reminiscent of excimer formation that is not observed here. Furthermore, we note that a similar effect is observed for  $C_{70}$  for which no excimer emission has been documented. Therefore, although we cannot completely exclude that the observed polarized emission component arises from the formation of excimer-like species, we attribute the observation of linear polarization from the encapsulated fullerene molecules to the local anisotropy induced by their environment that directly affects the  $S_1 \rightarrow S_0$  transition. To the best of our knowledge, this would represent the first observation of induced linear polarization in isolated fullerene chromophores.

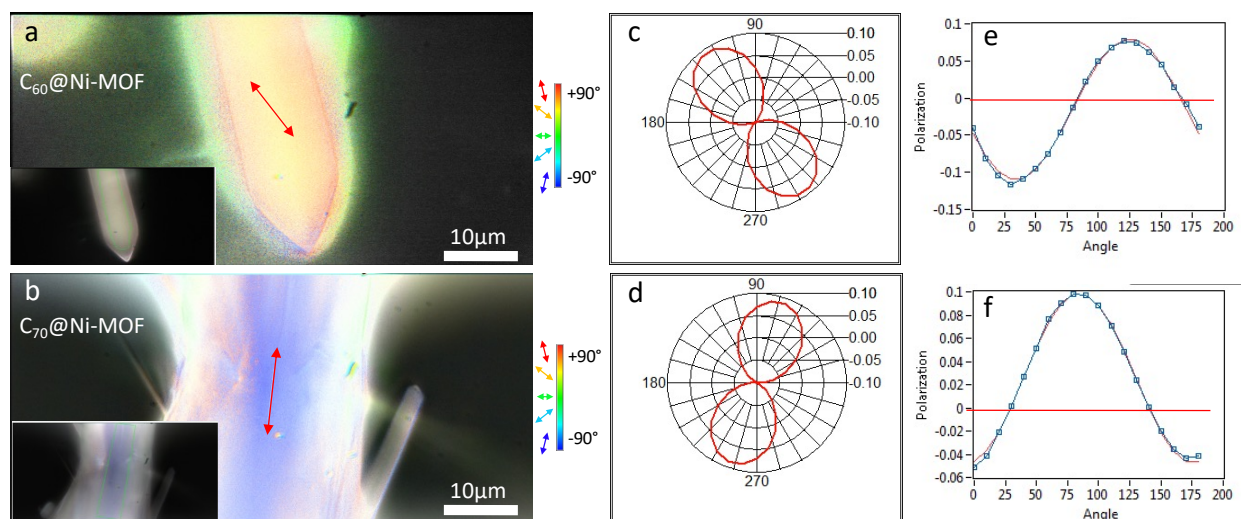


**Figure 5.** Confocal fluorescence microscopy images ( $\lambda_{\text{ex}} = 450 \text{ nm}$ ) showing the linear polarization component of the fullerene emission from **2** (a) and **3** (b). The red arrows indicate the orientation of the polarization shown in the polar plots of the angular dependence of the polarization  $P = (I_H - I_V) / (I_H + I_V)$ , V=vertical H=horizontal. for **2** (c, e) and **3** (d, f). Inset in (a) and (b) provides image at full-scale (+1, -1) polarization.

The analysis of the time-resolved emission decay from **3** and crystals of **1** encapsulating varying proportions of  $C_{60}$  and  $C_{70}$  solely evidences emission from  $C_{70}$ . This is indicative of either the occurrence of efficient energy transfer between the encapsulated fullerenes, or of selective uploading of  $C_{70}$  vs.  $C_{60}$ . Energy transfer from  $C_{60}$  to  $C_{70}$  is expected to be isoenergetic or slightly exoenergetic based on the relative energies of their  $S_0 - S_1$  transitions as determined from the onset of their absorption bands (2.0 vs. 1.9 kcal/mol for  $C_{60}$  and  $C_{70}$ , respectively).<sup>35</sup> Analysis of systems in which mixtures of fullerenes were encapsulated into **1** during the Ni-MOF was conducted by employing different binary ratios of  $C_{60}:C_{70}$  (90:10, 75:25, 50:50; 25:75, and 10:90) during the self-assembly process (Figure 6, S3, Table S2). In all of the mixed fullerene systems, only emission from  $C_{70}$  could be detected. Upon excitation at 450 nm, multi-exponential decays with  $\tau_{\text{avr.}} = 1.0$  and 1.1 ns were obtained for **2** and **3**, respectively. In contrast to energy transfer from excited anthracenes in the MOF scaffold to encapsulated  $C_{60}$  or  $C_{70}$ , where the distinct fullerene emission could be detected upon selective excitation of the anthracene donor, intra-fullerene energy

transfer is more difficult to ascertain due to the similarity in the absorption and emission spectra and kinetics. In the case of **1**, selective encapsulation of C<sub>70</sub> results in the enrichment of the hybrid material with the larger fullerene component.

**Fullerene separation.** Selective binding of fullerenes based on size complementarity has been previously documented in several covalent<sup>36–39</sup> and non-covalent<sup>40,41</sup> architectures and remains an attractive means of separating fullerene mixtures.<sup>42,43</sup> In some cases, preferential binding to C<sub>70</sub> was observed.<sup>37,44–47</sup> However, in spite of promising results, the synthesis of precisely engineered molecular and supramolecular components capable of distinguishing between fullerenes of different sizes is challenging. Instead, **1** is readily prepared on multi-gram scale using readily available components and could serve as an interesting platform for the construction of materials for fullerene separation. To evaluate this, the fullerene content of **1** exposed to different relative concentrations of C<sub>60</sub>/C<sub>70</sub> was analyzed by HPLC and mass spectrometry. Both techniques showed that the composition of the fullerene mixture trapped by the MOF is significantly enriched in C<sub>70</sub>. Based on this promising result, we proceeded to prepare a chromatography column packed with **1** as a stationary phase for the separation of fullerene mixtures. To this end, a stainless steel HPLC column (l = 150 mm, d = 10 mm) was packed with crystalline Ni-MOF **1** (10 g). One milligram of a commercially available fullerene mixture (MRT Ltd., 70% C<sub>60</sub>, 25% C<sub>70</sub>, 5% higher fullerenes) was dissolved in toluene and eluted with toluene through the column. The composition of the eluent was followed by collecting 5mL aliquots and analyzing each one by HPLC. After a first fraction in which the eluent composition contains 11% C<sub>70</sub>, the purity of the C<sub>60</sub> in the remaining fractions increased to 99±1 % indicating that the remaining C<sub>70</sub> was trapped on the column (Figure 6 and S7). In principle, bound C<sub>70</sub> can be easily separated from **L** and Ni<sup>2+</sup> by extraction in aqueous acid, thereby allowing recycling of the ligand.

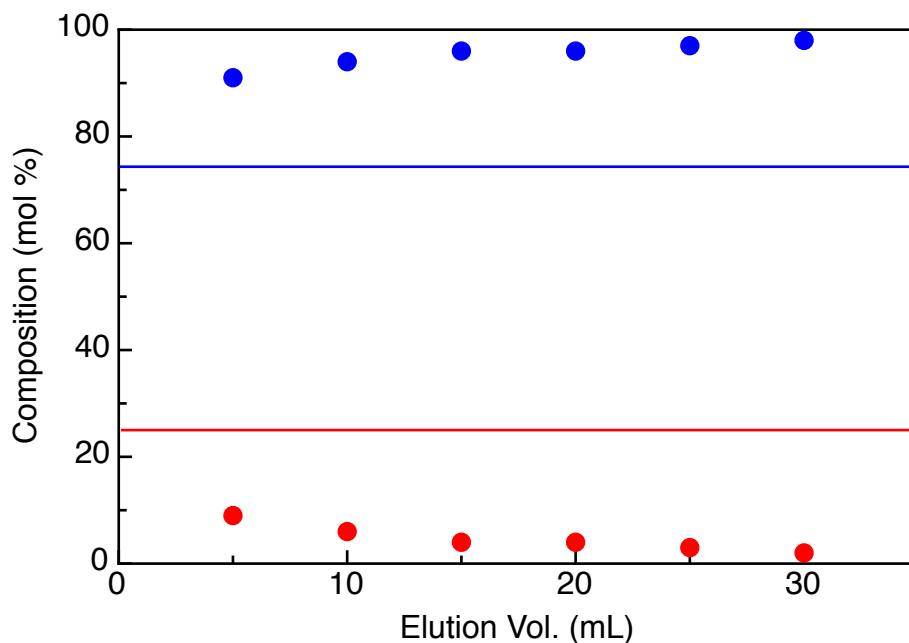


**Figure 6.** Molar fraction composition ( $C_{60}$ : blue circles;  $C_{70}$ , red circles) of fractions collected from a solution of fullerene mixture separated over an LC column packed with **1** as determined by HPLC (150 x 10 mm, eluent: toluene). The red and blue lines indicate the composition of the initial mixture in  $C_{70}$  and  $C_{60}$ , respectively.

## CONCLUSION

The straightforward preparation of **1** from readily available components allows easy access to a material presenting large channels able to incorporate  $C_{60}$ , and  $C_{70}$  guests during the self-assembly process. In contrast to fullerene loading through soaking, this was found to yield a homogeneous distribution of fullerenes inside the channels of the material as shown by both confocal Raman and fluorescence microscopy. The latter technique also evidences that the emission from encapsulated  $C_{60}$  is linearly polarized, which is unexpected from a chromophore possessing spherical symmetry. The absence of selective excitation suggests that the observed orientation of the transition dipole moment is due to environmental effects induced the

encapsulation inside the channels. These may also contribute to the observation of structured emission previously observed from with fullerenes at low temperature or in which the solvent molecules were frozen. Furthermore, **1** was found to present a higher affinity towards C<sub>70</sub> vs. C<sub>60</sub>, leading to its selective sequestration in fullerene mixtures in solution. A column packed with **1** is indeed able to afford a solution >99% C<sub>60</sub> when loaded with a mixture of fullerenes.

**Supporting information:** Crystallographic details, PXRD, Time-resolved spectra, Raman measurements, UV-Vis-NIR, HPLC fullerenes separation with Ni-MOF column, FT-IR and Thermal analysis. (PDF). The crystallographic data (CIFs) can be obtained free of charge from CSD using CCDC numbers for **1–3**: 1952043, 1977368, 1977380.

#### AUTHOR INFORMATION

Serhii I. Vasylevskyi [0000-0001-6219-6051](mailto:0000-0001-6219-6051)

Katharina M. Fromm [0000-0002-1168-0123](mailto:0000-0002-1168-0123)

Stefan Salentinig [0000-0002-7541-2734](mailto:0000-0002-7541-2734)

André Del Guerzo [0000-0003-1395-2302](mailto:0000-0003-1395-2302)

Dario M. Bassani [0000-0002-9278-1857](mailto:0000-0002-9278-1857)

Guillaume Raffy [0000-0002-8401-501X](mailto:0000-0002-8401-501X)

#### Corresponding Author

[serhii.vasylevskyi@gmail.com](mailto:serhii.vasylevskyi@gmail.com)

[dario.bassani@u-bordeaux.fr](mailto:dario.bassani@u-bordeaux.fr)

[katharina.fromm@unifr.ch](mailto:katharina.fromm@unifr.ch)

#### Present Addresses

† University of Fribourg, Chemistry Department, , Chemin Du Musee 9, Fribourg, 1700, Switzerland.

‡ University of Bordeaux, ISM CNRS UMR 5255, 33400 Talence, France

## Author Contributions.

**Serhii Vasylevskiy**<sup>†\*</sup>: Conceptualization, Methodology, Resources, Visualization, Validation, Formal Analysis, Funding acquisition, Investigation and Writing-Original Draft preparation.

**Guillaume Raffy**<sup>‡</sup> and **André Del Guerso**<sup>‡</sup>: Investigation, Visualization, Formal Analysis and Resources. **Stefan Salentinig**<sup>‡</sup>: Investigation, Visualization and Formal Analysis. **Katharina M.**

**Fromm**<sup>†\*</sup>: Writing-Reviewing & Editing, Funding acquisition, Resources and Project administration. **Dario M. Bassani**<sup>†\*</sup>: Conceptualization, Supervision, Project administration, Resources, Data Curation, Writing - Review & Editing and Funding Sources.

## Funding Sources

### ACKNOWLEDGMENT

We would like to acknowledge the University of Fribourg, the Swiss National Science Foundation SNSF, and the NCCR “Bioinspired Materials” as well as the Fribourg Centre for Nanomaterials FriMat for the support and opportunity to work under anthracene project. We thank Dr. Aurelien Crochet for the help with X-Ray diffraction methods and fruitful discussions. We appreciate support from the Adolphe Merkle Institute (AMI) for providing elemental analysis facilities. SV acknowledges the SNSF for granting a Doc.Mobility fellowship P1FRP2\_178150 to perform part of the work at the University of Bordeaux. This work was also supported by the ANR (ANR-17-CE24-0033), and the IDEX University of Bordeaux. We are grateful to the CESAMO for help with structural analyses.

### REFERENCES

- (1) Eddaoudi, M.; Kim, J.; Rosi, N.; Vodak, D.; Wachter, J.; O’Keeffe, M.; Yaghi, O. M. Hydrogen Storage in Microporous Metal-Organic Frameworks. *Science*. **2002**, *295*, 469–472.

- (2) Sudik, A. C.; Millward, A. R.; Ockwig, N. W.; Côté, A. P.; Kim, J.; Yaghi, O. M. Design, Synthesis, Structure, and Gas (N<sub>2</sub>, Ar, CO<sub>2</sub>, CH<sub>4</sub>, and H<sub>2</sub>) Sorption Properties of Porous Metal-Organic Tetrahedral and Heterocuboidal Polyhedra. *J. Am. Chem. Soc.* **2005**, *127*, 7110–7118.
- (3) Li, Q.-Y.; Ma, Z.; Zhang, W.-Q.; Xu, J.-L.; Wei, W.; Lu, H.; Zhao, X.; Wang, X.-J. AIE-Active Tetraphenylethene Functionalized Metal–Organic Framework for Selective Detection of Nitroaromatic Explosives and Organic Photocatalysis. *Chem. Commun.* **2016**, *52*, 11284–11287.
- (4) Esken, D.; Turner, S.; Wiktor, C.; Kalidindi, S. B.; Van Tendeloo, G.; Fischer, R. A. GaN@ZIF-8: Selective Formation of Gallium Nitride Quantum Dots inside a Zinc Methylimidazolate Framework. *J. Am. Chem. Soc.* **2011**, *133*, 16370–16373.
- (5) Jin, S.; Son, H. J.; Farha, O. K.; Wiederrecht, G. P.; Hupp, J. T. Energy Transfer from Quantum Dots to Metal-Organic Frameworks for Enhanced Light Harvesting. *J. Am. Chem. Soc.*, **2013**, *135*, 955–958.
- (6) Cui, Y.; Song, T.; Yu, J.; Yang, Y.; Wang, Z.; Qian, G. Dye Encapsulated Metal-Organic Framework for Warm-White LED with High Color-Rendering Index. *Adv. Funct. Mater.* **2015**, *25*, 4796–4802.
- (7) Lin, X.; Gao, G.; Zheng, L.; Chi, Y.; Chen, G. Encapsulation of Strongly Fluorescent Carbon Quantum Dots in Metal-Organic Frameworks for Enhancing Chemical Sensing. *Anal. Chem.* **2014**, *86*, 1223–1228.
- (8) Wu, Y. N.; Zhou, M.; Li, S.; Li, Z.; Li, J.; Wu, B.; Li, G.; Li, F.; Guan, X. Magnetic Metal-Organic Frameworks:  $\gamma$ -Fe<sub>2</sub>O<sub>3</sub>@MOFs via Confined in Situ Pyrolysis Method for Drug Delivery. *Small*. **2014**, *10*, 2927–2936.
- (9) Yuan, Z.; Zhang, L.; Li, S.; Zhang, W.; Lu, M.; Pan, Y.; Xie, X.; Huang, L.; Huang, W. Paving Metal-Organic Frameworks with Upconversion Nanoparticles via Self-Assembly. *J. Am. Chem. Soc.* **2018**, *140*, 15507–15515.
- (10) Quah, H. S.; Chen, W.; Schreyer, M. K.; Yang, H.; Wong, M. W.; Ji, W.; Vittal, J. J. Multiphoton Harvesting Metal-Organic Frameworks. *Nat. Commun.* **2015**, *6*, 1–7.
- (11) Zhuang, J.; Kuo, C.-H.; Chou, L.-Y.; Liu, D.-Y.; Weerapana, E.; Tsung, C.-K. Optimized Metal–Organic-Framework Nanospheres for Drug Delivery: Evaluation of Small-Molecule Encapsulation. *ACS Nano* **2014**, *8*, 2812–2819.
- (12) Zheng, H.; Zhang, Y.; Liu, L.; Wan, W.; Guo, P.; Nyström, A. M.; Zou, X. One-Pot Synthesis of Metal-Organic Frameworks with Encapsulated Target Molecules and Their Applications for Controlled Drug Delivery. *J. Am. Chem. Soc.* **2016**, *138*, 962–968.
- (13) Yan, D.; Tang, Y.; Lin, H.; Wang, D. Tunable Two-Color Luminescence and Host-Guest Energy Transfer of Fluorescent Chromophores Encapsulated in Metal-Organic Frameworks. *Sci. Rep.* **2014**, *4*, 4337.

- (14) Wei, Y.; Dong, H.; Wei, C.; Zhang, W.; Yan, Y.; Zhao, Y. S. Wavelength-Tunable Microlasers Based on the Encapsulation of Organic Dye in Metal-Organic Frameworks. *Adv. Mater.* **2016**, *28*, 7424–7429.
- (15) Rowsell, J. L. C.; Yaghi, O. M. Strategies for Hydrogen Storage in Metal-Organic Frameworks. *Angew. Chem. Int. Edit.* **2005**, *44*, 4670–4679.
- (16) Han, S. S.; Deng, W. Q.; Goddard, W. A. Improved Designs of Metal-Organic Frameworks for Hydrogen Storage. *Angew. Chem. Int. Edit.* **2007**, *46*, 6289–6292.
- (17) Han, S. S.; Mendoza-Cortés, J. L.; Goddard, W. A. Recent Advances on Simulation and Theory of Hydrogen Storage in Metal-Organic Frameworks and Covalent Organic Frameworks. *Chem. Soc. Rev.* **2009**, *38*, 1460–1476.
- (18) Yang, C. X.; Chen, Y. J.; Wang, H. F.; Yan, X. P. High-Performance Separation of Fullerenes on Metal-Organic Framework MIL-101(Cr). *Chem -Eur. J.* **2011**, *17*, 11734–11737.
- (19) Yang, C. X.; Yan, X. P. Selective Adsorption and Extraction of C70 and Higher Fullerenes on a Reusable Metal-Organic Framework MIL-101(Cr). *J. Mater. Chem.* **2012**, *22*, 17833–17841.
- (20) Goswami, S.; Ray, D.; Otake, K.; Kung, C.-W.; Garibay, S. J.; Islamoglu, T.; Atilgan, A.; Cui, Y.; Cramer, C. J.; Farha, O. K.; Hupp, J. T. A Porous, Electrically Conductive Hexa-Zirconium(IV) Metal–Organic Framework. *Chem. Sci.* **2018**, *9*, 4477–4482.
- (21) Meng, H.; Zhao, C.; Nie, M.; Wang, C.; Wang, T. Changing the Hydrophobic MOF Pores through Encapsulating Fullerene C60 and Metallofullerene Sc3C2@C80. *J. Phys. Chem. C.* **2019**, *123*, 6265–6269.
- (22) Chu, C. C.; Raffy, G.; Ray, D.; Guerzo, A. Del; Kauffmann, B.; Wantz, G.; Hirsch, L.; Bassani, D. M. Self-Assembly of Supramolecular Fullerene Ribbons via Hydrogen-Bonding Interactions and Their Impact on Fullerene Electronic Interactions and Charge Carrier Mobility. *J. Am. Chem. Soc.* **2010**, *132*, 12717–12723.
- (23) Chae, H. K.; Siberio-Pérez, D. Y.; Kim, J.; Go, Y.; Eddaoudi, M.; Matzger, A. J.; O’Keeffe, M.; Yaghi, O. M. A Route to High Surface Area, Porosity and Inclusion of Large Molecules in Crystals. *Nature.* **2004**, *427*, 523–527.
- (24) Liu, X.; Kozłowska, M.; Okkali, T.; Wagner, D.; Higashino, T.; Brenner-Weiß, G.; Marschner, S. M.; Fu, Z.; Zhang, Q.; Imahori, H.; Bräse, S.; Wenzel, W.; Wöll, C.; Heinke, L. Photoconductivity in Metal–Organic Framework (MOF) Thin Films. *Angew. Chem. Int. Edit.* **2019**, *58*, 9590–9595.
- (25) Viani, L.; Minoia, A.; Cornil, J.; Beljonne, D.; Egelhaaf, H. J.; Gierschner, J. Resonant Energy Transport in Dye-Filled Monolithic Crystals of Zeolite L: Modeling of Inhomogeneity. *J. Phys. Chem. C.* **2016**, *120*, 27192–27199.

- (26) Bossart, O.; De Cola, L.; Welter, S.; Calzaferri, G. Injecting Electronic Excitation Energy into an Artificial Antenna System through an Ru<sup>2+</sup> Complex. *Chem -Eur. J.* **2004**, *10*, 5771–5775.
- (27) Huo, Q.; Margolese, D. I.; Stucky, G. D. Surfactant Control of Phases in the Synthesis of Mesoporous Silica-Based Materials. *Chem. Mater.* **1996**, *8*, 1147–1160.
- (28) Sastre, G.; Cano, M. L.; Corma, A.; García, H.; Nicolopoulos, S.; González-Calbet, J. M.; Vallet-Regí, M. On the Incorporation of Buckminsterfullerene C<sub>60</sub> in the Supercages of Zeolite Y. *J. Phys. Chem. B.* **1997**, *101*, 10184–10190.
- (29) Li, H.; Hill, M. R.; Huang, R.; Doblin, C.; Lim, S.; Hill, A. J.; Babarao, R.; Falcaro, P. Facile Stabilization of Cyclodextrin Metal–Organic Frameworks under Aqueous Conditions via the Incorporation of C<sub>60</sub> in Their Matrices. *Chem. Commun.* **2016**, *52*, 5973–5976.
- (30) Wong, K. T.; Bassani, D. M. Energy Transfer in Supramolecular Materials for New Applications in Photonics and Electronics. *NPG Asia Mater.* **2014**, *6*, 116–116.
- (31) Razbirin, B. S.; Sheka, E. F.; Starukhin, A. N.; Nel'son, D. K.; Degunov, M. Y.; Shukov, I. V. Vibronic Resonance in Spectra of Frozen Solutions of the C<sub>60</sub> Fullerene Derivatives. *Phys. Solid State.* **2011**, *53*, 1307–1313.
- (32) Palewska, K.; Sworakowski, J.; Chojnacki, H.; Meister, E. C.; Wild, U. P. A Photoluminescence Study of Fullerenes: Total Luminescence Spectroscopy of C<sub>60</sub> and C<sub>70</sub>. *J. Phys. Chem.* **1993**, *97*, 12167–12172.
- (33) Sibley, S. P.; Argentine, S. M.; Francis, A. H. A Photoluminescence Study of C<sub>60</sub> and C<sub>70</sub>. *Chem. Phys. Lett.* **1992**, *188*, 187–193.
- (34) Raffy, G.; Ray, D.; Chu, C.-C.; Del Guerso, A.; Bassani, D. M. Controlling the Emission Polarization from Single Crystals Using Light: Towards Photopolic Materials. *Angew. Chem. Int. Edit.* **2011**, *50*, 9584–9588.
- (35) Kleineweischede, A.; Mattay, J. Photochemical Reaction of Fullerenes and Fullerene Derivatives. In *CRC Handbook of Photochemistry Organic and Photobiology*; Horspool, W., Lenci, F., Eds.; CRC Press: Boca Raton, USA, **2004**, *28*, 1-33.
- (36) Yang, Y. D.; Gong, H. Y. Thermally Activated Isomeric All-Hydrocarbon Molecular Receptors for Fullerene Separation. *Chem. Commun.* **2019**, *55*, 3701–3704.
- (37) Shi, Y.; Cai, K.; Xiao, H.; Liu, Z.; Zhou, J.; Shen, D.; Qiu, Y.; Guo, Q. H.; Stern, C.; Wasielewski, M. R.; Diederich, F.; Goddard, W. A.; Fraser Stoddart, J. Selective Extraction of C<sub>70</sub> by a Tetragonal Prismatic Porphyrin Cage. *J. Am. Chem. Soc.* **2018**, *140*, 13835–13842.
- (38) Ke, X. S.; Kim, T.; Brewster, J. T.; Lynch, V. M.; Kim, D.; Sessler, J. L. Expanded Rosarin: A Versatile Fullerene (C<sub>60</sub>) Receptor. *J. Am. Chem. Soc.* **2017**, *139*, 4627–4630.

- (39) Barendt, T. A.; Myers, W. K.; Cornes, S. P.; Lebedeva, M. A.; Porfyrakis, K.; Marques, I.; Félix, V.; Beer, P. D. The Green Box: An Electronically Versatile Perylene Diimide Macrocyclic Host for Fullerenes. *J. Am. Chem. Soc.* **2020**, *142*, 349–364.
- (40) Sun, W.; Wang, Y.; Ma, L.; Zheng, L.; Fang, W.; Chen, X.; Jiang, H. Self-Assembled Carcerand-like Cage with a Thermoregulated Selective Binding Preference for Purification of High-Purity C 60 and C 70. *J. Org. Chem.* **2018**, *83*, 14667–14675.
- (41) Martínez-Agramunt, V.; Gusev, D. G.; Peris, E. A Shape-Adaptable Organometallic Supramolecular Coordination Cage for the Encapsulation of Fullerenes. *Chem -Eur. J.* **2018**, *24*, 14802–14807.
- (42) Yi, H.; Zeng, G.; Lai, C.; Huang, D.; Tang, L.; Gong, J.; Chen, M.; Xu, P.; Wang, H.; Cheng, M.; Zhang, C.; Xiong, W. Environment-Friendly Fullerene Separation Methods. *Chem. Eng. J.* **2017**, *330*, 134–145.
- (43) García-Simón, C.; Costas, M.; Ribas, X. Metallosupramolecular Receptors for Fullerene Binding and Release. *Chem. Soc. Rev.* **2016**, *45*, 40–62.
- (44) Fang, X.; Zhu, Y. Z.; Zheng, J. Y. Clawlike Tripodal Porphyrin Trimer: Ion-Controlled on-off Fullerene Binding. *J. Org. Chem.* **2014**, *79*, 1184–1191.
- (45) Toyota, S.; Yamamoto, Y.; Wakamatsu, K.; Tsurumaki, E.; Muñoz-Castro, A. Nano-Saturn with an Ellipsoidal Body: Anthracene Macrocyclic Ring–C<sub>70</sub> Complex. *B. Chem. Soc. Jpn.* **2019**, *92*, 1721–1728.
- (46) Jiménez, V. G.; David, A. H. G.; Cuerva, J. M.; Blanco, V.; Campaña, A. G. A Macrocyclic Based on a Heptagon-Containing Hexa-*Peri*-hexabenzocoronene. *Angew. Chem. Int. Edit.* **2020**, *59*, 15124–15128.
- (47) Ni, Y.; Gordillo-Gómez, F.; Peña Alvarez, M.; Nan, Z.; Li, Z.; Wu, S.; Han, Y.; Casado, J.; Wu, J. A Chichibabin's Hydrocarbon-Based Molecular Cage: The Impact of Structural Rigidity on Dynamics, Stability, and Electronic Properties. *J. Am. Chem. Soc.* **2020**, *142*, 12730–12742.

TOC

